New Phytologist

Research

Methylated chalcones are required for rhizobial *nod* gene induction in the *Medicago truncatula* rhizosphere

Wenjuan Wu[1], Yuxin Zhuang[1], Dasong Chen[2], Yiting Ruan[1], Fuyu Li[1], Kirsty Jackson[3], Cheng-Wu Liu[4], Alison East[5], Jiangqi Wen[6], Evangelos Tatsis[1,3], Philip S. Poole[5], Ping Xu[7] and Jeremy D. Murray[1,3]

[1]National Key Laboratory of Plant Molecular Genetics, CAS-JIC Centre of Excellence for Plant and Microbial Science, Center for Excellence in Molecular Plant Sciences (CEMPS), Chinese Academy of Sciences, Shanghai, 200032, China; [2]State Key Laboratory of Agricultural Microbiology, College of Life Science and Technology, Huazhong Agricultural University, 1 Shizishan Street, Wuhan, 430070, China; [3]John Innes Centre, Norwich Research Park, Norwich, NR4 7UH, UK; [4]MOE Key Laboratory for Membraneless Organelles and Cellular Dynamics, School of Life Sciences, Division of Life Sciences and Medicine, University of Science and Technology of China, Hefei, 230026, China; [5]Department of Plant Sciences, University of Oxford, South Parks Road, Oxford, OX1 3RB, UK; [6]Institute for Agricultural Biosciences, Oklahoma State University, 3210 Sam Noble Parkway, Ardmore, OK 73401, USA; [7]Shanghai Collaborative Innovation Center of Plant Germplasm Resources Development, College of Life Sciences, Shanghai Normal University, 100 Guilin Road, Shanghai, 200234, China

Authors for correspondence:
Jeremy D. Murray
Email: jeremy.murray@jic.ac.uk

Ping Xu
Email: pingxu_ardnor@shnu.edu.cn

Received: *26 November 2023*
Accepted: *1 March 2024*

New Phytologist (2024) **242:** 2195–2206
doi: 10.1111/nph.19701

Key words: 4,4′-dihydroxy-2-methoxychalcone, bioreporter, chalcone-*O*-methyltransferases, flavonoids, host range, *Medicago truncatula*, NodD, nodulation.

Summary

- Legume nodulation requires the detection of flavonoids in the rhizosphere by rhizobia to activate their production of Nod factor countersignals. Here we investigated the flavonoids involved in nodulation of *Medicago truncatula*.
- We biochemically characterized five flavonoid-*O*-methyltransferases (OMTs) and a lux-based *nod* gene reporter was used to investigate the response of *Sinorhizobium medicae* NodD1 to various flavonoids.
- We found that chalcone-OMT 1 (ChOMT1) and ChOMT3, but not OMT2, 4, and 5, were able to produce 4,4′-dihydroxy-2′-methoxychalcone (DHMC). The bioreporter responded most strongly to DHMC, while isoflavones important for nodulation of soybean (*Glycine max*) showed no activity. Mutant analysis revealed that loss of ChOMT1 strongly reduced DHMC levels. Furthermore, *chomt1* and *omt2* showed strongly reduced bioreporter luminescence in their rhizospheres. In addition, loss of both ChOMT1 and ChOMT3 reduced nodulation, and this phenotype was strengthened by the further loss of OMT2.
- We conclude that: the loss of ChOMT1 greatly reduces root DHMC levels; ChOMT1 or OMT2 are important for *nod* gene activation in the rhizosphere; and ChOMT1/3 and OMT2 promote nodulation. Our findings suggest a degree of exclusivity in the flavonoids used for nodulation in *M. truncatula* compared to soybean, supporting a role for flavonoids in rhizobial host range.

Introduction

Most legumes engage in symbiotic interactions with soil bacteria called rhizobia which involves the attachment of rhizobia to root hair cells which then form a curl and entrap the rhizobia. Special transcellular structures called infection threads then form in the curled root hair and in underlying cells, providing passage for the rhizobia into a specialized root outgrowth called a nodule (Quilbé *et al.*, 2022; Wang *et al.*, 2022). The rhizobia are then endocytotically released from infection threads into nodule cells where they differentiate and fix atmospheric nitrogen into ammonia.

This symbiosis, referred to as nodulation, is highly specific, with certain species of rhizobia being able to colonize only a limited number of legume species. A major determinant of this specificity is Nod factors (NFs), the signaling molecules that are produced and released by the rhizobia and are perceived by the host plant. The binding of NFs to their cognate receptors triggers events leading to successful endosymbiotic infection and nodule formation (Broghammer *et al.*, 2012; Wang *et al.*, 2022). In this case, specificity is achieved through the production of NFs with specific modifications that activate the NF receptors of their compatible hosts (Downie, 1994; Radutoiu *et al.*, 2007; Luu *et al.*, 2022). This lock-and-key mechanism restricts the symbiotic interactions of each legume species to specific co-evolved rhizobia, thereby conferring a selective advantage to both partners (Walker *et al.*, 2020).

Nod factor production in rhizobia is triggered by flavonoids, a large class of phenolic compounds produced by plants. During nodulation, flavonoids are released from legume roots and activate the expression of rhizobial *nod* genes which encode the NF biosynthesis enzymes, as well as other genes important for nodulation, such as those encoding the type III secretion system in *Bradyrhizobium elkanii* (Bolzan de Campos *et al.*, 2011). The

response of rhizobia to flavonoids is mediated by the transcription factor NodD, which binds to the *nod*-box upstream of the *nod* gene operon to activate gene expression in a flavonoid-dependent manner (Spaink *et al.*, 1987; Yeh *et al.*, 2002). It has been demonstrated that the production of flavonoids by *Medicago truncatula* is essential for its nodulation by *Sinorhizobium meliloti* (Wasson *et al.*, 2006). Besides being essential for nodulation, rhizobial studies indicate that flavonoids may also play an important role in host specificity. This is suggested by the observation that in many cases different flavonoids induce the *nod* genes of rhizobia that nodulate different hosts (Liu & Murray, 2016; Wang *et al.*, 2018; Walker *et al.*, 2020). For instance, *nod* gene reporter activity in *Bradyrhizobium japonicum* USDA110, which nodulates soybean (*Glycine max*), is strongly activated by the isoflavones genistein and daidzein, but not in response to the chalcone 4,4′-dihydroxy-2′-methoxychalcone (DHMC; Banfalvi *et al.*, 1988). Conversely, *S. meliloti* NodD1 mediates *nod* gene activation in the presence of DHMC, but not with genistein or daidzein (Peck *et al.*, 2006; Kamboj *et al.*, 2010). This specificity is typically reflected by the ability of root exudates to induce *nod* gene expression. For example, the NodD from *Mesorhizobium ciceri*, which nodulates chickpea (*Cicer arietinum*), mediates expression from a *nod* gene reporter in the presence of chickpea root exudates, but not those of alfalfa, clover (*Trifolium pratense*), or pea (*Pisum sativum*; Kamboj *et al.*, 2010). It was also shown that other compounds, such as trigonelline and stachydrine, can act as *nod* gene inducers in *S. meliloti* (Phillips *et al.*, 1992). Importantly, several reports have shown that transfer of *nodD* genes can alter rhizobial host range. Substitution of the *nodD* of *R. trifolii* strain ANU851 with that of either *R. leguminosarum* or *S. meliloti* narrowed its host range, allowing nodulation of *Trifolium repens* (white clover) but not *T. pratense* (red clover) (Spaink *et al.*, 1987). A *Sinorhizobium meliloti* strain carrying the nodD1 of the *Rhizobium* strain MPIK3030 enabled it to nodulate the nonhost *Macroptilium atropurpureum* (Horvath *et al.*, 1987). The addition of the *nodD1* from *R. leguminosarum trifolii* ANU843 to *Rhizobium* NGR234 extends its host range to the nonlegume *Parasponia andersoni* (Bender *et al.*, 1988). Transfer of *R. tropici* CIAT 899 *nodD1* to *R. etli* and *R. leguminosarum* sv. *trifolii*, extended their host range to *Leucaena esculents and Phaseolus vulgaris*, respectively (Sousa *et al.*, 1993). Regardless, while data from rhizobial studies indicate that flavonoids play a role in specificity, genetic evidence is needed to determine the extent of this role and to identify which flavonoids, or other compounds, are needed for the nodulation of specific legumes.

Genetic studies in three different legume species have provided some progress in identifying host flavonoids involved in nodulation. In soybeans, RNAi was used to reduce the expression of *Isoflavone Synthase*, suggesting that the isoflavones daidzein and genistein are important for nodulation in this species (Subramanian *et al.*, 2006). In *L. japonicus*, reduced nodulation was seen with RNAi-suppression of *Chalcone Isomerase 4* (*CHI4*) transcripts, suggesting that flavanones play a role in this interaction (Kelly *et al.*, 2018). Finally, RNAi-based knockdown of two flavone synthases, which produce 7,4′-dihydroxyflavone (DHF), reduced nodulation in *M. truncatula* (Zhang *et al.*, 2007, 2009). It was previously shown that the flavone DHF can induce *nod* genes of both soybean and *Medicago* symbionts (Kosslak *et al.*, 1987; Maxwell *et al.*, 1989), so it is possible that multiple legumes use DHF for nodulation. On the other hand, genistein or daidzein can induce the expression of *nod* gene reporters in *Bradyrhizobium japonicum* but not in *S. meliloti*, suggesting that it's unlikely that isoflavonoids are important for the nodulation of alfalfa or *M. truncatula* (Peck *et al.*, 2006; Kamboj *et al.*, 2010). Clearly, more genetic data is needed to ascertain whether different legumes use different flavonoids, which ones are important for nodulation, and to what extent they determine the rhizobial host range.

In *Medicago sativa*, another root flavonoid, DHMC, was shown to have stronger *nod* gene-inducing activity than DHF (Maxwell *et al.*, 1989). Investigations by Maxwell *et al.* (1992, 1993) in *M. sativa* revealed that DHMC is produced by chalcone-*O*-methyltransferase (MsChOMT) through methylation of isoliquiritigenin. Subsequent determination of the MsChOMT crystal structure and functional analysis of the protein was used to identify specific residues involved in substrate binding (Zubieta *et al.*, 2001; Noel *et al.*, 2003). Later studies showed that several *MsChOMT* homologs in *M. truncatula* were symbiotically induced, some of which were shown to be specifically expressed in infected root hairs during rhizobial infection and in young nodules (Breakspear *et al.*, 2014; Chen *et al.*, 2015). Although genetic evidence to support DHMC's role in nodulation is missing, its strong *nod* gene-inducing activity and its association with rhizobial infection indicate its potential importance.

In this study, we show that two MsChOMT homologs from *M. truncatula* catalyze the production of DHMC and these, along with another homolog of unknown function, are required for nodulation of *M. truncatula*. We use a lux-based rhizobia reporter strain to show that loss of the major isoform of ChOMT reduces DHMC to nearly undetectable levels and greatly reduces *nod* gene activation in the *M. truncatula* rhizosphere. Using the same reporter strain we confirm that genistein and daidzein, which are known to activate *nod* genes in *B. japonicum*, do not activate expression of *S. meliloti nod* genes. Our findings indicate that soybean and *M. truncatula* use different flavonoids for nodulation, suggesting a role for these compounds in host specificity.

Materials and Methods

Plant material

Medicago truncatula Gaertn. ecotype R108 was used as WT depending on the experiments. The following *Tnt1* insertion mutants were obtained from the mutant resource at Oklahoma State University, USA: *chomt1-1* (from line NF10582), *chomt1-2* (NF12032) and *chomt1-3* (NF16030); *omt2-1* (NF5164) and *omt2-2* (NF4653).

GUS analysis

The creation of the promoter: β-glucoronidase (GUS) constructs for *OMT2* (originally named *ChOMT2* in Chen *et al.*, 2015) and

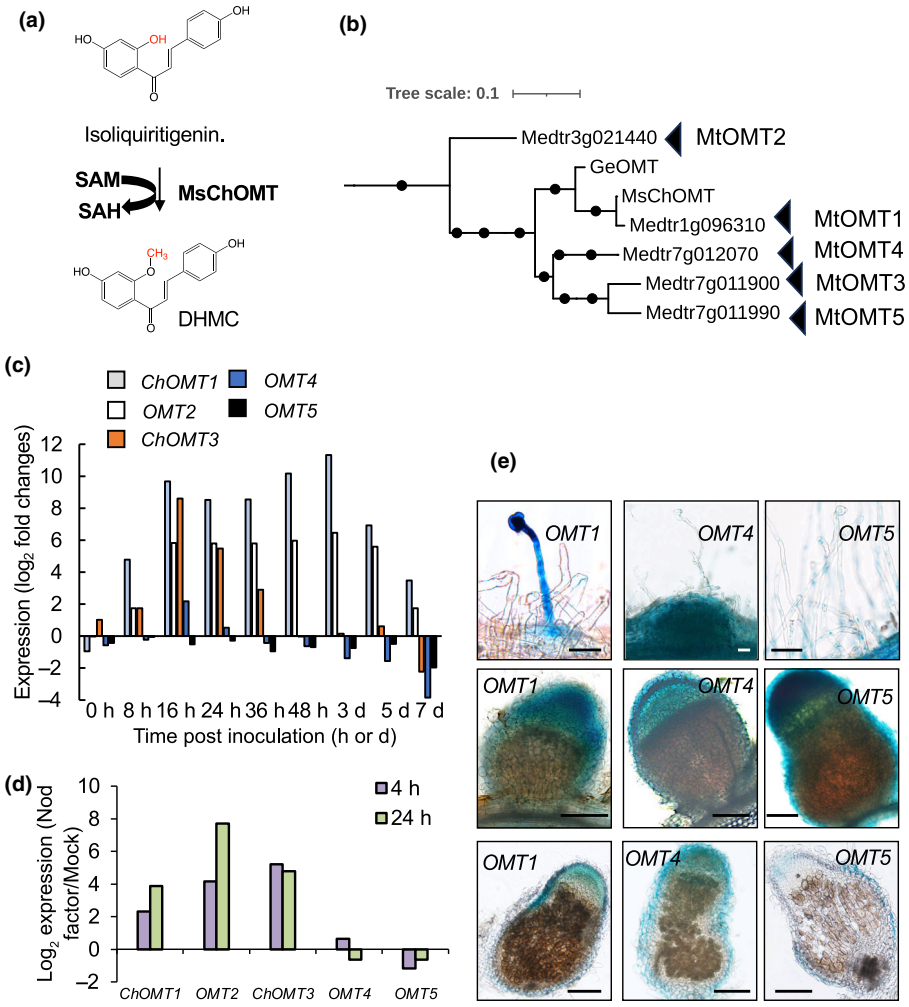

Fig. 1 The phylogenetic relationship between chalcone-*O*-methyltransferase (MsChOMT) and its closest *Medicago truncatula* homologs and their expression patterns during nodulation. (a) The methylation of isoliquiritigenin catalyzed by MsChOMT. (b) A portion of the phylogenetic tree of *M. truncatula* OMTs (Supporting Information Fig. S3) shows the clade containing the proteins of interest. MsChOMT from *M. sativa* (alfalfa) and GeOMT from *Glycyrrhiza echinata* (licorice) were included for comparison. Branches with bootstrap support > 0.80 are marked with a black dot. (c) Expression of *M. truncatula OMT*s at *Sinorhizobium meliloti* spot inoculation sites. Data from Schiessl *et al*. (2019). (d) *OMT* expression levels in *M. truncatula* in root hair cells 4 and 24 h after treatment with Nod factors (NFs). Data from Jardinaud *et al*. (2016). (e) p*ChOMT1*, p*OMT4* and p*OMT5* GUS-reporter analysis of transgenic roots 7–21 days post inoculation (dpi) with *S. meliloti* 2011. Arrows indicate rhizobia-induced root hair curls. Top row: root hairs and nodule primordia 7 dpi; bottom two rows: mature nodules 21 dpi. The bottom row shows *c*. 50 μm nodule sections. Bars: (top panel) 50 μm; (middle and bottom panels) 200 μm.

OMT3/*ChOMT3* was previously described (Chen *et al*., 2015). The promoter region of *OMT4* (from 0 to −2053 bp) was synthesized by Genescript. The promoters of *ChOMT1* (Medtr1g096310; from −108 to −2027 bp) and *OMT5* (Medtr7g011990; from 0 to −2393 bp) were amplified by PCR and cloned into pENTR. Then, LR reactions were performed to insert the promoter regions upstream of GUS in the pKGWFS7 vector using the GATEWAY cloning system (Life Technologies). The primers used for amplification are listed in Supporting Information Table S1. *M. truncatula* R108 seedlings were transformed with the various constructs using *Agrobacterium rhizogenes*-mediated hairy root transformation (Chabaud *et al*., 2006). After growth on Fahräeus medium plates (Barker *et al*., 2006), composite plants with transgenic roots were transferred to a nitrogen-free soil mixture and inoculated with *S. meliloti* 2011, and watered as needed. Nodulated roots were then stained for GUS activity at 7, 14 or 21 d post-inoculation (dpi). For GUS analysis, excised roots were stained with 0.5 mg ml^{-1} 5-bromo-4-chloro-3-indolyl β-D-glucuronide, cyclohexylammonium salt, X-Gluc) (X-GlcA; Yeasen Biotechnology Co., Ltd., China) as previously described (Stomp, 1992), and incubated at 37°C for 1–3 h. Stained nodules were vibratome sectioned, rinsed with water, and fixed in 70% ethanol before imaging.

Overexpression of *ChOMT1* and *OMT3*/*ChOMT3*

Constructs for overexpression of *ChOMT1* and *OMT3*/*ChOMT3* were constructed using Golden Gate cloning. The CDS of *ChOMT1* and *OMT3*/*ChOMT3* were individually inserted into the pL0V-SC-41308 entry vector. Vector pL1V-F2-47742 was used as a backbone to generate a Level 1 (L1) constructs from the L0 constructs containing the *Lotus japonicus* (Regel) K. Larsen *Ubiquitin* (*LjUBI*) promoter (pL0M-PU-LjUBI1-15 251) and *OMT* CDS (pL0V-SC-41308), and pL0M-T-H4-15323. Vector pL1V-R1-47802 was used as a backbone to generate a construct for expressing dsRed from the 35S promoter, containing pL0M-PU-p35S-15 058, pL0M-SC-dsRed-15 073 and pL0M-T-Ocs-1-41 432. Finally, L2 constructs for overexpression of *ChOMT1* and *ChOMT3* (pLjUBI-ChOMT1-H4-p35S-dsRed-Ocs-ELE2 and pLjUBI-ChOMT3-H4-p35S-dsRed-Ocs-ELE2) were introduced into *A. rhizogenes* using hairy root transformation.

Quantitative real-time polymerase chain reaction

The RNA extraction was carried out using the Total RNA Extraction Kit (Tiangen, Beijing, China). Quantitative real-time polymerase chain reaction was carried on an Applied

Biosystems™ 7500 Real-Time PCR System, using 2× Realstar green fast mixture with ROX (GenStar). In each case, three biological replicates each with three technical replicates were used. *M. truncatula Ubiquitin* was used as a housekeeping gene. The expression was then calculated relative to the control using the $\Delta\Delta C_t$ method. Primer specificity was checked on a 2% agarose gel containing ethidium bromide. The primers used are listed in Table S1.

Protein expression and *in vitro* enzyme assays

The CDS of *ChOMT1*, *OMT2*, *OMT3*/*ChOMT3*, *OMT4*, and *OMT5* were inserted between the *Kpn* I and *Hind* III restriction sites of the pOPINF vector (His-tag) using the In-Fusion® HD Cloning Kit as directed by the manufacturer (Takara Bio USA, San Jose, CA, USA), and then transferred into *Escherichia coli* DH5α. All primers used in vector construction are listed in Table S1. Transformants were plated on LB containing carbenicillin and single colonies were picked and sequence verified. Plasmids containing the correct inserts were transferred to *E. coli* BL21 (DE3) for protein expression. Protein expression was induced by 0.5 mM isopropyl β-D-thiogalactoside and incubation was carried out for 16 h at 18°C, starting from an OD_{600} of 0.8. The cells were harvested and the proteins were purified using QIAGEN Ni-NTA Agarose. Ten μg of each protein was loaded on an 8% SDS-PAGE gel and run at 150 V for 1.5 h followed by fast Coomassie Blue staining.

The enzymatic reaction systems (100 μl) contained 200 ng μl^{-1} recombinant protein, 500 μM S-adenosyl-L-methionine (SAM), 100 μM isoliquiritigenin, 10 mM phosphate buffer (pH 7.5), and dH_2O. The reactions were incubated at 25°C for 2 h and stopped by the addition of 100 μl of 100% methanol. Kinetic assays were performed in 100 μl final volume reactions containing 100 nM protein, 250 μM SAM, and 10 mM phosphate buffer (pH 7.5) and were incubated at 25°C for 20 min with concentrations of isoliquiritigenin varying from 3.125 to 200 μM. The reaction mixture for kinetic assays was extracted twice using methanol (1 : 1 volume) with centrifugation at 13 500 ***g*** for 10 min, and the supernatant was passed through a 0.22 μm filter and then analyzed using an AB SCIEX 6500+ LC-MS/MS system. The reaction products were quantified using a DHMC standard curve. V_{max}, K_m, and K_{cat} values were calculated using the Michaelis–Menten equation in GraphPad Prism 8 software.

High-performance liquid chromatography (HPLC) analysis

The above enzyme reaction products were analyzed using an Ultimate Ultra 3000 chromatography system (Thermo Fisher Scientific, Waltham, MA, USA). A 250 mm × 4.6 mm, 5 μm particle size C18 column (Thermo Fisher Scientific) was used for chromatographic separation at RT with a flow rate of 0.3 ml min^{-1}. Gradient elution was performed as follows: water containing 0.1% formic acid (A) and acetonitrile (B), 0 min, 25% B; 0–8 min, 25–75% B; 9–12 min, 75–95% B; 12–13 min, 95% B, 13–16 min, 95–25% B. The injection volume was 10 μl and the UV detection wavelength was 346 nm.

Creation of the flavonoid bioreporter and *lux* assays

The flavonoid bioreporter plasmid pLMB830 was created by cloning a 1384 bp PCR product amplified from the region upstream of pSMED_RS30380 (*nodA*) containing all of its regulator and SMED_RS30375 (*nodD1*) of *Sinorhizobium medicae* WSM419 into *Xho*I-digested pIJ11268. The predicted *S. medicae* and *S. meliloti* NodD1 sequences differ by only six amino acids and their predicted flavonoid binding regions (as described in Ferguson *et al.*, 2020) are 100% identical. The pLMB830 plasmid was then transferred into *S. meliloti* 2011 by triparental mating (Pini *et al.*, 2017). The *S. meliloti* 2011/pLMB830 bacteria were cultured in 100 ml freshly prepared UMS liquid medium (Pini *et al.*, 2017) with 10 mg l^{-1} tetracycline and grown at 28°C for 24–36 h. A version of the reporter lacking *nodD1* was unable to respond to flavonoids, indicating that assays using pLMB830 reflect the activity of the plasmid-borne copy of *S. medicae* NodD1 (Fig. S1).

For flavonoid assays in liquid culture, 1, 10 and 100 nM of different flavonoids were added to an $OD_{600} = 0.2$ culture of *S. meliloti* 2011/pLMB830 and after 8 h at 28°C (OD_{600} of *c.* 1.0). The flavonoids used are shown in Fig. S2. Then 200 μl of the bacteria was transferred to transparent 96 well plates and luminescence was measured using a Varioskan Flash Spectral Scanning Multimode Reader (Thermo Fisher Scientific).

For analysis of bioreporter luminescence on roots, *M. truncatula* seeds were scarified, sterilized, and imbibed and then transferred onto agarose plates placed nearly vertically in growth chambers (23°C with a 16 h : 8 h, day : night cycle) for 3 d. The *S. meliloti* 2011/pLMB830 culture was prepared essentially as described above, 2–5 ml of bacteria were grown to an OD_{600} of 0.6–0.8 in UMS medium. The rhizobia were pelleted and the pellet was washed using dH_2O and then resuspended in dH_2O to a final OD_{600} of *c.* 0.05. Then 10 μl of the rhizobia was inoculated directly onto each plant near the root tip. Plates were then placed in a near-vertical position in a growth chamber. A NightShade LB 985 *In vivo* imaging system (Berthold Technologies, Bad Wildbad, Germany) was used to take pictures of the plates at 2 and 7 dpi. CCD bright field images were exposed for 0.1 s and for luminescence signal acquisition 120-s exposures were used. Images were analyzed with the IndiGO imaging software. Total root luminescence was determined for each seedling. At least fifteen seedlings per line were analyzed for each treatment.

Extraction and analysis of flavonoids

Seedlings were grown in a growth chamber in nitrogen-free soil for 4 d and then half the plants were inoculated with *S. meliloti* 2011 and watered as needed. Three days later both groups of seedlings were put into aluminum foil-covered tubes (seven seedlings per tube) containing 5 ml of Fahräeus medium. After 8 h the plants were removed and the root exudates were lyophilized. Then, the dried samples were extracted using 100 μl of 80% methanol followed by sonication for 10 min. Then the mixtures were centrifuged twice at 13 500 ***g*** for 15 min to remove any precipitates and the final supernatants were transferred into glass

vials before LC-MS/MS analysis. For root extracts, excised roots were ground to a fine powder using liquid nitrogen and then extracted with 80% methanol solution (v/w, 5 : 1) at RT for 3 h. Then the mixtures were centrifuged twice at 13 500 ***g*** for 15 min to remove precipitates and the supernatants were transferred into glass vials before LC-MS/MS analysis. Five to six replicates were used for each sample.

Quantification of plant flavonoids

Following extraction, flavonoids were analyzed by liquid chromatography-tandem mass spectrometry using an AB SCIEX 6500+ LC-MS/MS system using negative mode ionization. An Agilent InfinityLab Poroshell 120 SB-Aq column (3 × 100 mm, 2.7 µm particle size) with a flow rate of 400 µl min^{-1} and an injection volume of 3 µl was used to separate analytes. The column oven was set at 30°C and the autosampler at 4°C. Two mobile phases (A: 0.01% formic acid and 2 mM ammonium formate in water and B: 100% methanol) were used in the LC method. A linear gradient program was used as follows: 0–1 min, 20% B; 1–15.5 min, 20–60% B; 15.5–16 min, 60–95% B, 16–18 min, 95% B, 18–18.1 min, 95–20% B, 18.1–20 min, 20% B. The injection volume was 3 µl. The instrument parameters were as follows: curtain gas, 35 psi; collision gas, medium; temperature, 500°C; ion source gas 1, 50 psi; ion source gas 2, 50 psi; and ion spray voltage, −4500 V.

CRISPR/Cas9 knockouts in hairy roots

The pKGSD401-p35S: Cas9 vector containing dsRed as a transgenic marker was used for the CRISPR-knockout experiments (Jiang *et al.*, 2021). The guide RNAs were designed using CRISPR-P 2.0 (Liu *et al.*, 2017). Two gRNAs for two target sites with pG-T1T2 (gRNA scaffold) overhangs were designed as forward and reverse primers, and pG-T1T2 was used as a template for amplifying gRNA scaffold as described in Xing *et al.* (2014). The final pKGSD401 constructs were introduced into *M. truncatula* seedlings using hairy root transformation (Chabaud *et al.*, 2006). Plant genomic DNA was extracted for genotyping. PCR fragments containing the target sites were amplified from the gDNA of transformed hairy roots and were sequenced. The sequencing results were analyzed using CRISP-ID to characterize CRISPR-mediated indels and substitutions (Dehairs *et al.*, 2016).

Nodulation assays

For nodulating the mutants, *S. meliloti* 2011/*hemA:lacZ* was grown overnight in TY medium to an OD_{600} of 0.8–1.0 and then was pelleted and then resuspended in dH_2O to an OD_{600} of 0.02 and 1 ml of the rhizobia per plant was used to inoculate 7-d-old *M. truncatula* seedlings. Nodules were then scored at 21 dpi. For hairy root composite plants, roots lacking dsRed fluorescence were removed and the seedlings with dsRed positive roots were moved to a vermiculite: perlite mixture (1 : 1) without nitrogen. Plants were inoculated with *S. meliloti* 2011/*hemA:lacZ* after 3 d in soil, and then dsRed positive roots were scored for nodules at 21 dpi.

In silico gene expression analysis and phylogenetic tree construction

In silico gene expression analysis was carried out using the Noble MtGEA V3 by LIPME (Benedito *et al.*, 2008) and MtExpress V2 (Carrere *et al.*, 2021). Pfam search was used to identify the OMT dimerization and *O*-methyltransferase domains. Phylogenetic analysis was performed using the Phylogeny.fr 1-click phylogeny pipeline with the default parameters and displayed using ITOL (Dereeper *et al.*, 2008; Letunic & Bork, 2021). All gene IDs and synonyms for genes in this study are provided in Table S2.

Bacterial strains used in this study

Sinorhizobium meliloti 2011 carrying the pXLGD4 (*hemA:lacZ*) plasmid was used for nodulation phenotyping experiments. *S. meliloti* carrying pLMB830 (*nodD1-nodA:luxCDABE*) was used for all luminescence experiments.

Results

Identification of symbiotic *OMT*s in *M. truncatula*

Medicago truncatula homologs of MsChOMT, which catalyses the methylation of isoliquiritigenin (Fig. 1a), were identified using BLAST. This revealed 48 full-length homologs that contained both dimerization and *O*-methyltransferase domains, including one (Medtr1g096310) sharing 98.6% amino acid identity, which was designated as ChOMT1. These sequences, along with GeOMT from *Glycyrrhiza echinata* (licorice), which can methylate licodione at the 2′-hydroxy position (Ichimura *et al.*, 1997), and MsChOMT were used to construct a phylogenetic tree. This analysis showed that MsChOMT, MtChOMT1, and GeOMT fall within a clade of five *M. truncatula* homologs (Fig. 1b, full tree shown in Fig. S3). Six of these homologs are clustered within a *c.* 110 kb interval on chromosome 7 (Fig. S4a). Further analysis using the closest homologs from nonlegume species showed that these OMTs belong to a larger legume-specific clade that is absent from apple (*Malus domestica*) and oak (*Quercus rubra*; Fig. S4b), suggesting that they are legume-specific. Notably, the six-gene cluster in *M. truncatula* appears to have arisen recently, as *Glycine soja* and *L. japonicus* have only one copy, and *Lens culinaris*, which is a member of the IRLC clade like *M. truncatula*, has only two copies at this locus.

To identify *OMT*s with potential roles in nodulation we investigated their expression under symbiotic conditions using data available in MtExpress (Carrere *et al.*, 2021). This revealed that the close homologs *ChOMT1*, *OMT3* (Medtr7g011900), and *OMT4* (Medtr7g012070), and the slightly more distantly related *OMT2* (Medtr3g021440), are induced at rhizobial spot inoculation sites (Fig. 1c). *ChOMT1* and *OMT2* showed high induction throughout the 5 d infection period while *OMT3* induction was

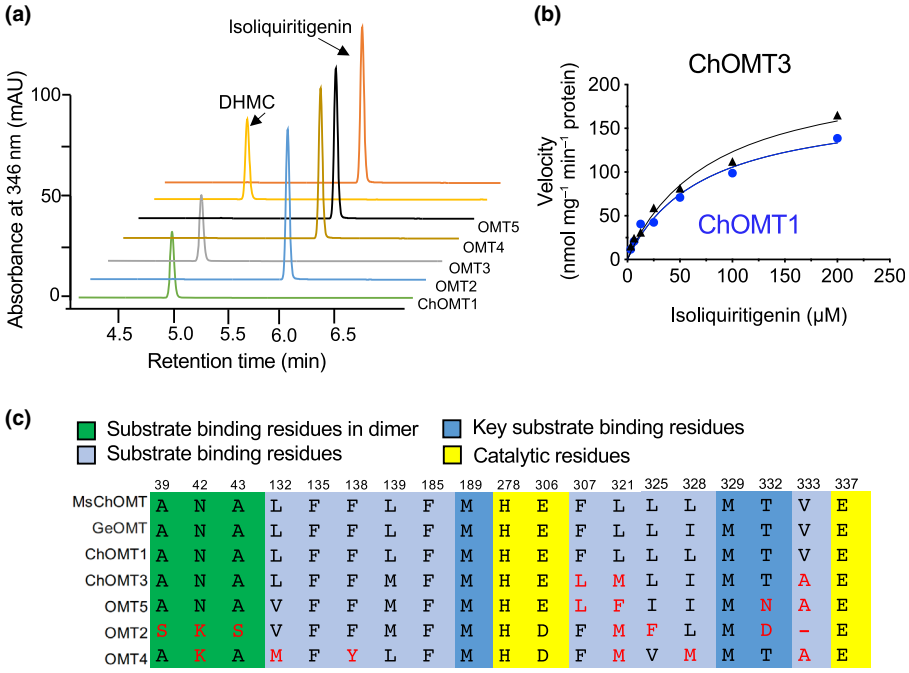

Fig. 2 Isoliquiritigenin methyltransferase activity assays for *Medicago truncatula* OMTs. (a) High-performance liquid chromatography traces of OMT assay products with isoliquiritigenin supplied as the substrate. Isoliquiritigenin and 4,4′-dihydroxy-2′-methoxychalcone standards are indicated. (b) Michaelis–Menten curve for ChOMT1 (circles) and ChOMT3 (triangles). (c) Protein haplotype of key OMT residues (Zubieta *et al*., 2001; Noel *et al*., 2003). Numbering based on chalcone-*O*-methyltransferase (MsChOMT). Nonconserved amino acids relative to MsChOMT are shown in red.

Table 1 Kinetic parameters of recombinant ChOMT1 and ChOMT3 using isoliquiritigenin as substrate.

Enzyme	K_m (μM)	V_{max} (nmol mg^{-1} min^{-1})	K_{cat} (s^{-1})
ChOMT1	71.5 ± 18.66	181.0 ± 20.44	0.12 ± 0.014
ChOMT3	80.9 ± 18.45	222.5 ± 22.85	0.15 ± 0.016

limited to the earliest stages (8–36 hpi) of infection (data from Schiessl *et al*., 2019). All four of these genes were also induced in epidermal cells by NFs (Fig. 1d) (Jardinaud *et al*., 2016). *OMT4* showed only weak induction under both treatments. Besides these, *OMT5* (Medtr7g011990), which is highly expressed in root hairs but is not induced by rhizobia or NFs, was also investigated.

The spatial expression patterns of *OMT2* and *OMT3* during nodulation were previously investigated by Chen *et al*. (2015) and were found to be expressed in rhizobia-infected root hairs, throughout the nodule primordia (NP), and in the apex of mature nodules. We then investigated the spatiotemporal expression patterns of the remaining three homologs in nodulated *M. truncatula* roots using promoter-GUS analysis (pChOMT1-, pOMT4-, pOMT5-GUS) using *A. rhizogenes* hairy root transformation. This revealed that *ChOMT1* was specifically expressed in infected root hairs, while *OMT4* and *OMT5* were expressed in both infected and uninfected root hairs. *ChOMT1*, *OMT4* and *OMT5* were also expressed in young developing nodules and in the nodule apex of mature nodules, but not in the interzone or nitrogen fixation zone (Fig. 1e). These data suggest that these *OMTs* could be involved in rhizobial infection.

ChOMT1 and OMT3 are isoliquiritigenin OMTs

ChOMT1 and OMT2-5 belong to the same phylogenetic clade as MsChOMT and GeOMT, which were reported to, respectively, methylate isoliquiritigenin and licodione at the 2′-hydroxy position (Ayabe *et al*., 1980; Maxwell *et al*., 1992). To investigate the biochemical function of ChOMT1, it was heterologously expressed in *E. coli* as a His-tagged protein, purified, and then incubated with isoliquiritigenin to analyze its activity (Fig. S5a). High-performance liquid chromatography analysis of the reaction products showed a new peak 1 (p1) with a retention time of 4.8 min and a UV absorption peak of 346 nm (Fig. S5b). Mass spectrometry of peak 1 (p1) gave a precursor ion $[M–H]^-$ at *m/z* (mass to charge ratio of the ions) 269.0819, indicating a methyl group was added to isoliquiritigenin (*m/z* 255.0663) (Fig. S5c). The p1 compound was then examined using ^{1}H NMR, ^{1}H NMR (500 MHz, Methanol-d4): δ 7.64–7.55 (m, 2H), 7.53 (d, J = 8.6 Hz, 2H), 7.43 (d, J = 15.7 Hz, 1H), 6.84 (d, J = 8.6 Hz, 2H), 6.54 (d, J = 2.2 Hz, 1H), 6.48 (dd, J = 8.5, 2.2 Hz, 1H), 3.91 (s, 3H) (Fig. S5d). The ^{1}H NMR profile of the product is in good accordance with that of DHMC (Maxwell *et al*., 1989; Lee, 2011). The other purified OMT proteins were similarly tested for their activity against isoliquiritigenin (Fig. S5a). Of these, only OMT3 showed activity and was renamed as ChOMT3 (Fig. 2a). Under optimal conditions (25°C, pH 7.5), ChOMT1 exhibited Km values of 71.51 μM and its K_{cat} was 0.12 s^{-1}. ChOMT3 exhibited Km values of 80.88 μM and its K_{cat} was 0.15 s^{-1} (Fig. 2b; Table 1). This indicates that ChOMT1 has a stronger substrate binding affinity while ChOMT3 has a higher catalytic efficiency. Given the high degree of sequence similarity between ChOMT1/3 and GeOMT, we tested their activity, as well as OMT2/4, against licodione (Fig. S6). Both ChOMT1 and ChOMT3 were able to methylate licodione, but appeared to be selective for isoliquiritigenin, while GeOMT showed only minor activity against both substrates, and OMT2/4 showed no activity.

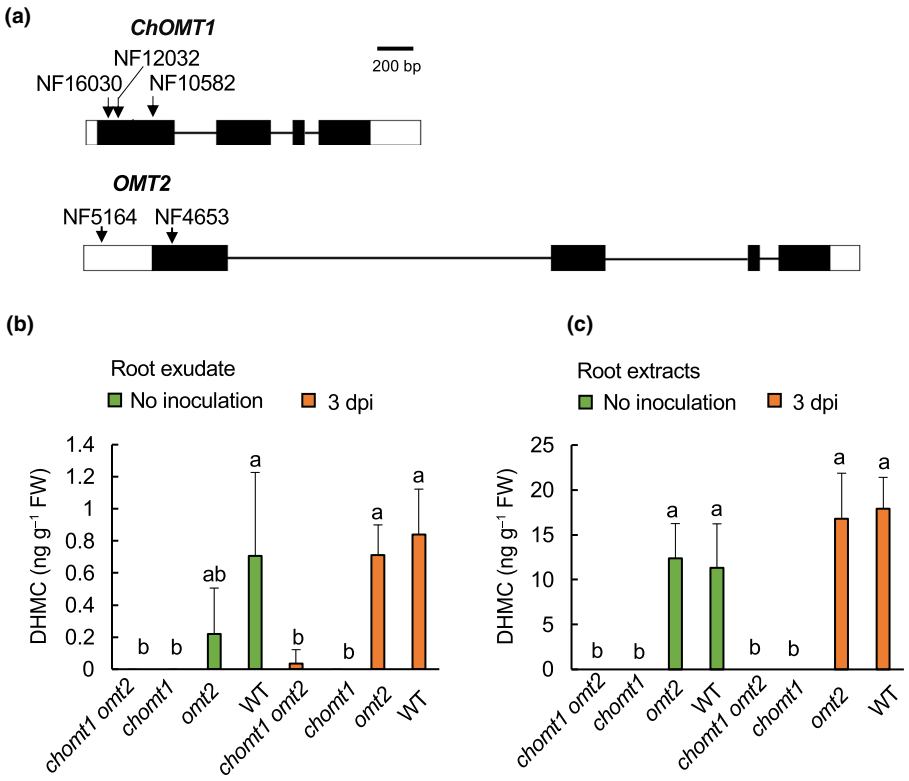

Fig. 3 Flavonoid content of *chomt1* and *omt2* mutants. (a) Gene structure of *Medicago truncatula ChOMT1* and *OMT2* with *Tnt1* transposon insertion positions indicated by arrows. NF10582 (*chomt1-1*), NF12032 (*chomt1-2*), and NF16030 (*chomt1-3*). *OMT2*, *omt2-1* (NF5164) and *omt2-2* (NF4653). Black boxes: exons, black lines: introns, and white boxes: 5′ and 3′ UTRs. The 4,4′-dihydroxy-2′-methoxychalcone content in (b) root exudates and (c) root extracts of wild-type (R108) and *chomt1-2* and *omt2-2* single mutants and *chomt1-3 omt2-2* double mutants. Means were compared using Tukey's test ($P < 0.05$). Error bars ±SD. $n = 4$, with 7 seedlings per biological replicate. Roots were harvested at 3 d post-inoculation (dpi) with *Sinorhizobium meliloti* 2011 or noninoculated plants at the same time point.

To investigate the functional relationships of ChOMT1/3, and OMT2/4/5, their catalytic and substrate binding residues were predicted based on alignment with MsChOMT, which was extensively characterized by (Zubieta *et al.*, 2001). The authors reported that methylation of isoliquiritigenin by MsChOMT involves the catalytic residues His278, Glu306 and Glu337. The conservation of these three residues (Fig. 2c), as well as the SAM binding domain (not shown), in all five enzymes, suggests they are functional methyltransferases. Three key substrate binding residues, Met189, Met329 and Thr332, which ensure the A-ring 2′-hydroxy is firmly positioned for deprotonation and methylation, were conserved in all of these except for OMT2/5. This is consistent with the ChOMT1/3 and GeOMT being 2′-*O*-methyltransferases and suggests that OMT2/5 have different regioselectivity. Finally, the substrate binding residues in the dimer interface (Ala39, Asn42, Ala43) were conserved in ChOMT1/3 and OMT5 but differed in OMT2/4, indicating they may have different substrates (Fig. 2c).

ChOMT1 is responsible for most DHMC biosynthesis in *M. truncatula* roots

To further study the role of OMTs that are induced during nodulation, we obtained *Tnt1* mutants for *ChOMT1* and *OMT2*. For ChOMT1, homozygous mutants were isolated from lines NF10582 (*chomt1-1*, insertion at position 395), NF12032 (*chomt1-2*, insertion at position 95 bp), and NF16030 (*chomt1-3*, insertion at position 43 bp). For *OMT2*, *omt2-1* (NF5164) and *omt2-2* (NF4653) had insertions at −361 bp and 63 bp, respectively (Fig. 3a). No mutants with insertions in *ChOMT3* were found. We then isolated *chomt1* and *omt2* homozygotes and generated a *chomt1-3 omt2-2* double mutant by crossing. We then directly assayed the levels of flavonoids in mutant and wild type (WT) roots and root exudates using LC-MS/MS with and without rhizobial inoculation. Consistent with earlier reports in alfalfa (Maxwell & Phillips, 1990), we found that DHMC levels in exudates of rhizobia-inoculated WT plants showed a small nonsignificant increase compared to controls (Fig. 3b). The same trend was seen for DHMC in root extracts and the increase was more pronounced ($P = 0.13$, Tukey's test; Fig. 3c). A severe drop in DHMC, to nearly undetectable levels, was seen in *chomt1-2* and the *chomt1-3 omt2-2* double mutant root exudates and root extracts regardless of inoculation status, while DHMC levels in *omt2* were similar to WT (Fig. 3b,c). The levels of isoliquiritigenin, the precursor of DHMC, in root exudates and extracts appeared slightly increased in the mutants in some cases, but the changes were not significant (Fig. S7a,b).

ChOMT1, OMT2 and ChOMT3 promote nodulation

We then tested the importance of ChOMT1 and OMT2 for nodulation. We found that the number of nodules and infection threads was unaffected in the *chomt1-1,2,3*, *omt2-1,2*, and *chomt1-3 omt2-2* mutants (Fig. S8a–d). This could be caused by functional redundancy of other homologs, particularly ChOMT3 which showed similar activity against isoliquiritigenin as ChOMT1. Thus, the role of ChOMT3 was further investigated. We used CRISPR/Cas9 technology using two guide RNAs to

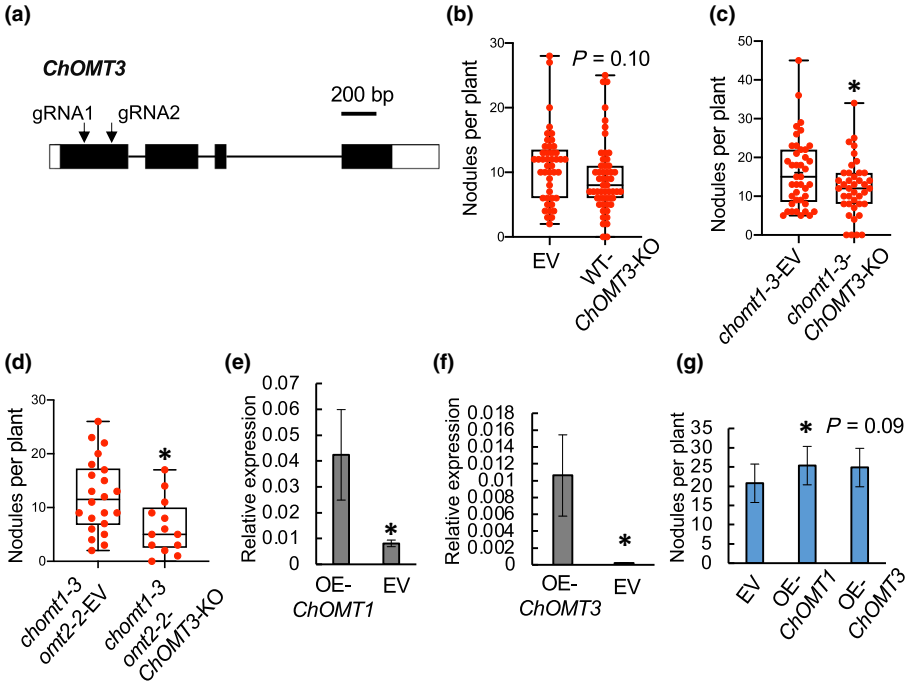

Fig. 4 *ChOMT1*, *ChOMT3*, and *OMT2* promote nodulation of *Medicago truncatula*. (a) gRNAs targeting *ChOMT3* for CRISPR/Cas9 mediated knockouts in *A. rhizogenes* hairy roots are indicated by arrowheads. (b) Nodule number of wild-type (R108) plants transformed with empty vector (EV) and *ChOMT3*-knockout (*ChOMT3*-KO) plants 21 d post-inoculation (dpi) with *Sinorhizobium meliloti* strain 2011. For EV $n = 45$, and for *chomt3*, $n = 53$. (c) Nodule number of *chomt1*/EV plants and *chomt1*/*ChOMT3*-KO plants 21 dpi with *S. meliloti* strain 2011. For *chomt1*/EV $n = 27$, and for *chomt1*/*ChOMT3*-KO $n = 20$. (d) Nodule number of *chomt1-3 omt2-2*/EV plants and *chomt1-3 omt2-2*/*ChOMT3-KO* plants at 21 dpi with *S. meliloti* strain 2011. EV $n = 22$, for *chomt1-3 omt2-2*/*ChOMT3-KO* $n = 13$. (e) Relative expression of *ChOMT1* in pro*LjUBI-ChOMT1* (OE-*ChOMT1*) transformed hairy roots. (f) Relative expression of *ChOMT3* in pro*LjUBI-ChOMT3* (OE-*ChOMT3*) transformed hairy roots. Expression values were determined by quantitative real-time polymerase chain reaction and expressed relative to *Ubiquitin*. EV, roots transformed by empty vector control. (g) Nodule number in pro*LjUBI-ChOMT1* and pro*LjUBI-ChOMT3* transformed hairy roots at 21 dpi with *S. meliloti* strain 2011. For EV $n = 46$, for pro*LjUBI-ChOMT1* $n = 47$, and for pro*LjUBI-ChOMT3* $n = 49$. Error bars ±SE from three biological replicates in (e–g). In (b–d) the box indicates the first to third quartile, the line indicates the median, and the whiskers indicate the minimum and maximum. In (b–g) means were compared using Student's *t*-test: *, $P < 0.05$.

target the first exon of *ChOMT3* (*ChOMT3*-KO) (Fig. 4a). WT roots transformed with *ChOMT3*-KO showed a slight, nonsignificant ($P = 0.10$), decrease in nodule number compared to the empty vector (EV) transformed control (Fig. 4b). We then transformed the *ChOMT3*-KO construct into the *chomt1* mutant background. Sequencing of PCR products from genomic DNA of the *chomt1 ChOMT3*-KO transgenic roots revealed mutations in 20 of the 23 transgenic hairy roots for the first guide RNA and 1 of 11 transgenic hairy roots for the second position guide RNA. The overall mutation frequency of *ChOMT3* was 87.0% (Fig. S8e). Only roots with mutations in *ChOMT3* were scored for nodulation. The *chomt1 ChOMT3*-KO roots showed a reduction in nodule number compared with the *chomt1* control roots (EV) at 21 dpi (Fig. 4c). Finally, we introduced *ChOMT3*-KO into the *chomt1-3 omt2-2* mutant, which resulted in a strong reduction of nodulation (Fig. 4d).

To further test the roles of *ChOMT1* and *ChOMT3*, we overexpressed them using the *L. japonicus* ubiquitin promoter (pro*LjUBI-ChOMT1* and pro*LjUBI-ChOMT3*) in *M. truncatula* hairy roots. Quantitative real-time polymerase chain reaction showed that *ChOMT1* and *ChOMT3* were successfully overexpressed in the transgenic roots (Fig. 4e, f). The p*LjUBI-ChOMT1* and p*LjUBI-ChOMT3* roots formed 20% and 22% more nodules than control roots at 21 dpi with *S. meliloti* 2011, respectively, but only the former was significant (Fig. 4g). Our results suggest that ChOMT1, ChOMT3 and OMT2 promote nodulation in *M. truncatula*.

chomt1 and *omt2* roots have reduced *nod* gene-inducing flavonoids in their rhizospheres

A previous report showed that *Rhizobium leguminosarum* carrying a *lux* operon driven by the *nodA* promoter was able to detect flavonoids in the rhizosphere and nodules of pea (Pini *et al.*, 2017). In *S. medicae*, the *nod* gene operon is activated by the NodD1 protein in a flavonoid-dependent manner (Mulligan & Long, 1985; Peck *et al.*, 2006). We created a flavonoid bioreporter by placing the genomic fragment containing the entire *nodD1* CDS and promoter and the adjacent *nodA* promoter upstream of the *lux* operon (*S. meliloti*/*nodD1-nodA:luxCDABE*). We then inoculated WT and mutant roots with the bioreporter strain to test its utility to detect *nod* gene-inducing flavonoids *in vivo*. This reporter was active on WT *M. truncatula* roots, showing luminescence around the root tips, while the *chomt1*, *omt2*, and *chomt1 omt2* plants showed strongly reduced luminescence (Fig. 5a,b). In addition, luminescence was detected in nodules of WT,

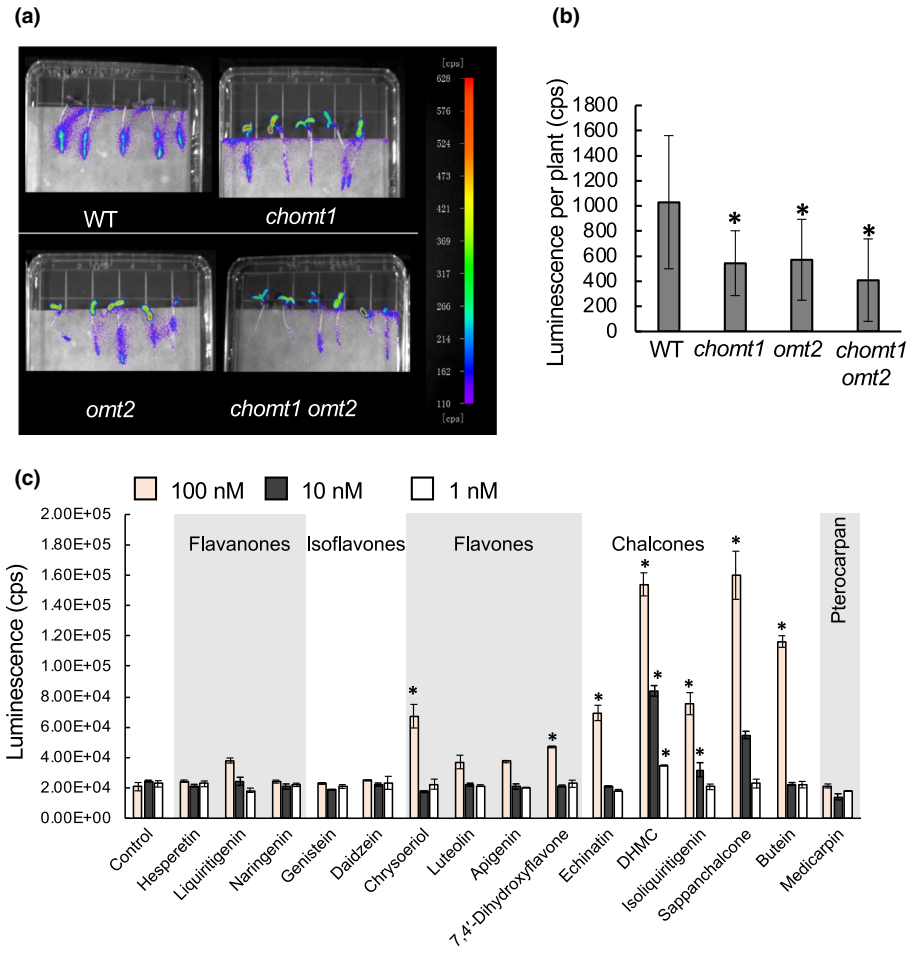

Fig. 5 *ChOMT1* and *OMT2* are important for *nod* gene induction in the *Medicago truncatula* rhizosphere. (a) Luminescence signal in plant rhizosphere of wild-type (WT) (R108), *chomt1-1*, *omt2-1* and *chomt1-3 omt2-2* double mutants 2 d post-inoculation (dpi) with *Sinorhizobium meliloti* 2011/pLMB830. (b) Quantification of luminescence signal in (a). For WT $n = 28$; *chomt1-1* $n = 15$, *omt2-2* $n = 25$, and *chomt1-3 omt2-2* double mutants $n = 19$. Student's *t*-test (*, $P < 0.05$). Error bars ±SD. (c) Luminescence of *S. meliloti* 2011/pLMB830 incubated with 1, 10 and 100 nM flavonoids in liquid culture for 12 h. cps, counts per second. *, $P < 0.05$ level (Dunnett's test). Error bars ±SD.

chomt1, and *chomt1 omt2* at 7 dpi (Fig. S9a), but no obvious differences in intensity were seen. Notably, many of the plants, including uninoculated plants, showed photoluminescence in the green tissues and the bioreporter strain did not show luminescence in the absence of plants (Fig. S9b). Based on these findings we conclude that *chomt1*, *omt2*, and *chomt1 omt2* mutants secrete lower levels of *nod* gene-inducing flavonoids at their root apices, while no obvious difference in this activity was observed in their nodules.

DHMC is a strong *nod* gene inducer

We then tested the ability of several flavonoids to activate the *S. meliloti* 2011/pLMB830 bioreporter in a liquid culture assay. We tested flavonoids that were reported to be present in *M. truncatula* root exudates, isoliquiritigenin, liquiritigenin, DHF, and DHMC, as well as those found in *M. truncatula* roots, including apigenin, naringenin, and medicarpin. We also included chrysoeriol and luteolin, which are found in *M. truncatula* seed coats, and several chalcones, echinatin (an isomer of DHMC), and butein and sappanchalcone, which have 2′hydroxy and methoxy groups, respectively. Finally, we included daidzein and genistein, which are the primary *nod* gene inducers for the soybean symbiont, *B. japonicum* (Subramanian *et al.*, 2006), and hesperetin, a strong *nod* gene inducer for the pea symbiont *R. leguminosarum* (Firmin *et al.*, 1986; Begum *et al.*, 2001). At 100 nM five chalcones (DHMC, sappanchalcone, butein, isoliquiritigenin, and echinatin) and two flavones (chrysoeriol and DHF) significantly induced luminescence (Fig. 5c). At 10 nM, only DHMC, sappanchalcone, and isoliquiritgenin showed activity, and only DHMC was able to induce luminescence at 1 nM.

Our results show that the *S. meliloti* 2011/pLMB830 reporter is preferentially activated by chalcones and suggest that DHMC is the strongest *S. medicae nod* gene inducer in *M. truncatula* root exudates.

Discussion

The activation of rhizobial *nod* genes by host flavonoids triggers the nodulation process. Here we show that the loss of *ChOMT1* results in a decrease of *nod* gene-inducing flavonoids in the *M. truncatula* rhizosphere. We further found that ChOMT1 and ChOMT3 produce the strong *nod* gene inducer DHMC and that their activity, along with OMT2, promotes nodulation of *M. truncatula*.

The bioreporter described herein was able to detect flavonoids in the rhizosphere as well as in liquid culture, where it was sensitive down to nanomolar levels. Using this reporter we observed a pattern of activity for *M. truncatula* as that described for an *R. leguminosarum*-based reporter on *Pisum sativum* and *Vicia sativa*:

a strong signal was seen at the root tip that gradually disappeared after rhizobial inoculation and reappeared in nascent nodules (Pini *et al.*, 2017). Our assays using purified flavonoids showed that *S. medicae* NodD1 responds strongly to chalcones, especially those with 2′-hydroxy or methyl groups, with DHMC having the strongest activity. By contrast, the reporter was insensitive to isoflavonoids that were shown to act as *nod* gene inducers in *B. japonicum* and are required for nodulation of soybean (Kosslak *et al.*, 1987; Subramanian *et al.*, 2006). Consistent with this, available transcriptome data indicate that soybean *ChOMT* homologs are not induced by *B. japonicum* (Libault *et al.*, 2010), further suggesting that DHMC is unlikely to play a role in soybean nodulation. Conversely, genistein and daidzein do not activate the *nod* genes of other rhizobia, such as *S. meliloti*, *R. leguminosarum* sv. *trifolii*, and *R. leguminosarum* sv. *viciae* (Kamboj *et al.*, 2010 and this study), suggesting that different legumes use different flavonoids for nodulation. On the other hand, good activity of the bioreporter was also seen with the flavone DHF, which was previously implicated in nodulation of *M. truncatula* (Zhang *et al.*, 2009), indicating that DHF and DHMC both contribute to nodulation in *M. truncatula*. Notably, the greatly diminished DHMC content of *chomt1* was associated with a halving of *nod* gene-inducing activity in root tips; whether DHF contributes to the remaining activity is unknown.

Our study demonstrates that methylation of chalcones enhances their *nod* gene-inducing activity, with DHMC and sappanchalcone, which are 2′-methylated, having stronger activities than their respective counterparts isoliquiritigenin and butein, which have 2′-hydroxy groups (structures in Fig. S2). Methylation could affect flavonoid bioactivity by improving membrane permeability, by enhancing their transport (either secretion by the plant and/or uptake by the rhizobia; Fang *et al.*, 2017), or by improved binding/activation of the NodD protein. In legumes flavonoid malonylation and glutathionation have been shown to be important for their transport across membranes and flavonoid malonylation was shown to promote nodulation (Li *et al.*, 1997; Zhao *et al.*, 2011; Ahmad *et al.*, 2021; Darwish *et al.*, 2022). In animal cells, improved intestinal absorption and persistence of methylated flavonoids were observed compared to their unmethylated counterparts, suggesting that methylation improves the bioavailability and stability of these compounds (Wen & Walle, 2006). Hence, OMTs, which substitute more reactive hydroxyl groups for more stable methyl groups, might improve the metabolic stability of flavonoids in biological systems, and so may enhance their persistence in the rhizosphere.

Studies have revealed that plant OMTs methylate a wide range of compounds with a high degree of selectivity (Liu *et al.*, 2022). Zubieta *et al.* (2001) reported the crystal structures of ChOMT and IOMT from *M. sativa*. The authors reported that the active site residues donated from partner monomers upon dimerization provide a protein–protein interface that contributes to substrate binding (Noel *et al.*, 2003). Our comparative analysis revealed that MsChOMT, ChOMT1/3 and GeOMT, which can methylate the 2′-hydroxy group of isoliquiritigenin, show conservation of the residues of the substrate binding domain in the dimer interface and active site donated from partner monomers. MtOMT2/4/5, which varied at these sites, were not active against isoliquiritigenin, suggesting their substrates differ. OMT2/5 also vary from ChOMT1/3 at the Thr332 position, a key substrate binding residue that ensures that the A-ring 2′-hydroxy is firmly positioned for deprotonation and methylation, suggesting they have different regioselectivity. Identification of the OMT2/4/5 substrates would help further reveal the structure–function relationships of this important class of enzymes.

OMT2 showed no activity against isoliquiritigenin or licodione, consistent with it having different predicted substrate binding residues than ChOMT1/3. When inoculated with the bioreporter, the *omt2* mutant unexpectedly showed a strongly reduced signal in rhizobia-inoculated roots, similar to that seen with *chomt1*, indicating that OMT2 is involved in the production of an *S. medicae nod* gene inducer. However, the *nod* gene activation phenotypes of *chomt1*, *omt2* and the *chomt1 omt2* double mutant were similar, suggesting that ChOMT1 and OMT2 may act in the same pathway, perhaps to further methylate DHMC. However, while our analysis suggested that OMT2 has different regioselectivity, it was unable to methylate DHMC (data not shown) and DHMC levels, which in this case might be expected to increase in *omt2*, were unchanged. Metabolic profiling of the *omt2* mutant and transgenic overexpression of OMT2 could help clarify the role of this enzyme.

This study demonstrates that DHMC serves as a key activator of *S. medicae nod* gene expression in the rhizosphere and suggests that it is specifically and locally produced in symbiotically infected cells. Finally, while Nod factors are understood as the principal factor determining specificity, our findings suggest that the recognition of specific flavonoids by rhizobia acts as a second constraint for compatibility. Hence, flavonoids, through their direct regulation of Nod factor production, appear to serve as specificity multipliers.

Acknowledgements

This research was supported by funding from the National Natural Science Foundation of China (32150710527), The Ministry of Science and Technology (2019FA0904703), Shanghai Science and Technology Commission (22JC1410800), and Shanghai Engineering Research Center of Plant Germplasm Resources (17DZ2252700). We would like to acknowledge Yisheng Wang for technical support.

Competing interests

None declared.

Author contributions

WW, PX and JDM conceived and designed the study; experiments were mainly conducted by WJ with contributions from CL, YZ, YR DC, AE, LF and KJ; PSP, AE and YR created the bioreporter strain; JW provided the *Tnt1* mutants; JDM, WW and PX wrote the manuscript; ET provided expert guidance and material support for the NMR and enzyme assays.

ORCID

Cheng-Wu Liu https://orcid.org/0000-0002-6650-6245
Jeremy D. Murray https://orcid.org/0000-0003-3000-9199
Evangelos Tatsis https://orcid.org/0000-0002-4013-1537
Wenjuan Wu https://orcid.org/0000-0002-3020-6988
Ping Xu https://orcid.org/0000-0001-9031-9004

Data availability

All data are available in the Supporting Information.

References

Ahmad MZ, Zhang Y, Zeng X, Li P, Wang X, Benedito VA, Zhao J. 2021. Isoflavone malonyl-CoA acyltransferase GmMaT2 is involved in nodulation of soybean by modifying synthesis and secretion of isoflavones. *Journal of Experimental Botany* **72**: 1349–1369.

Ayabe S-I, Yoshikawa T, Kobayashi M, Furuya T. 1980. Biosynthesis of a retrochalcone, echinatin: involvement of O-methyltransferase to licodione. *Phytochemistry* **19**: 2331–2336.

Banfalvi Z, Nieuwkoop A, Schell M, Besl L, Stacey G. 1988. Regulation of *nod* gene expression in *Bradyrhizobium japonicum*. *Molecular Genetics and Genomics* **214**: 420–424.

Barker DG, Pfaff T, Moreau D, Groves E, Ruffel S, Lepetit M, Whitehand S, Maillet F, Nair RM, Journet E-P. 2006. Growing *M. truncatula*: choice of substrates and growth conditions. In: Mathesius U, Journet EP, Sumner LW, eds. *The* Medicago truncatula *handbook*. Ardmore, OK, USA: The Samuel Roberts Noble Foundation, e1–26.

Begum AA, Leibovitch S, Migner P, Zhang F. 2001. Specific flavonoids induced nod gene expression and pre-activated nod genes of *Rhizobium leguminosarum* increased pea (*Pisum sativum* L.) and lentil (*Lens culinaris* L.) nodulation in controlled growth chamber environments. *Journal of Experimental Botany* **52**: 1537–1543.

Bender G, Nayudu M, Le Strange K, Rolfe B. 1988. The *nodD1* gene from *Rhizobium* strain NGR234 is a key determinant in the extension of host range to the nonlegume *Parasponia*. *Molecular Plant–Microbe Interactions* **1**: 259–266.

Benedito VA, Torres-Jerez I, Murray JD, Andriankaja A, Allen S, Kakar K, Wandrey M, Verdier J, Zuber H, Ott T *et al.* 2008. A gene expression atlas of the model legume *Medicago truncatula*. *The Plant Journal* **55**: 504–513.

Bolzan de Campos S, Deakin WJ, Broughton WJ, Passaglia LMP. 2011. Roles of flavonoids and the transcriptional regulator TtsI in the activation of the type III secretion system of *Bradyrhizobium elkanii* SEMIA587. *Microbiology (Reading)* **157**: 627–635.

Breakspear A, Liu C, Roy S, Stacey N, Rogers C, Trick M, Morieri G, Mysore KS, Wen J, Oldroyd GE *et al.* 2014. The root hair "infectome" of *Medicago truncatula* uncovers changes in cell cycle genes and reveals a requirement for Auxin signaling in Rhizobial infection. *Plant Cell* **26**: 4680–4701.

Broghammer A, Krusell L, Blaise M, Sauer J, Sullivan JT, Maolanon N, Vinther M, Lorentzen A, Madsen EB, Jensen KJ *et al.* 2012. Legume receptors perceive the rhizobial lipochitin oligosaccharide signal molecules by direct binding. *Proceedings of the National Academy of Sciences, USA* **109**: 13859–13864.

Carrere S, Verdier J, Gamas P. 2021. MtExpress, a comprehensive and curated RNAseq-based gene expression atlas for the model legume *Medicago truncatula*. *Plant & Cell Physiology* **62**: 1494–1500.

Chabaud M, Boisson-Dernier A, Zhang J, Taylor CG, Yu O, Barker DG. 2006. *Agrobacterium rhizogenes*-mediated root transformation. In: Mathesius U, Journet EP, Sumner LW, eds. *The* Medicago truncatula *handbook*. Ardmore, OK, USA: The Samuel Roberts Noble Foundation, e1–8.

Chen DS, Liu CW, Roy S, Cousins D, Stacey N, Murray JD. 2015. Identification of a core set of rhizobial infection genes using data from single cell types. *Frontiers in Plant Science* **6**: 575.

Darwish DBE, Ali M, Abdelkawy AM, Zayed M, Alatawy M, Nagah A. 2022. Constitutive overexpression of GsIMaT2 gene from wild soybean enhances rhizobia interaction and increase nodulation in soybean (*Glycine max*). *BMC Plant Biology* **22**: 431.

Dehairs J, Talebi A, Cherifi Y, Swinnen JV. 2016. CRISP-ID: decoding CRISPR mediated indels by Sanger sequencing. *Scientific Reports* **6**: 28973.

Dereeper A, Guignon V, Blanc G, Audic S, Buffet S, Chevenet F, Dufayard JF, Guindon S, Lefort V, Lescot M *et al.* 2008. PHYLOGENY.FR: robust phylogenetic analysis for the non-specialist. *Nucleic Acids Research* **36**: W465–W469.

Downie JA. 1994. Signalling strategies for nodulation of legumes by rhizobia. *Trends in Microbiology* **2**: 318–324.

Fang Y, Cao W, Xia M, Pan S, Xu X. 2017. Study of structure and permeability relationship of flavonoids in Caco-2 Cells. *Nutrients* **9**: 1301.

Ferguson S, Major AS, Sullivan JT, Bourke SD, Kelly SJ, Perry BJ, Ronson CW. 2020. *Rhizobium leguminosarum* bv. trifolii NodD2 enhances competitive nodule colonization in the clover-rhizobium symbiosis. *Applied and Environmental Microbiology* **86**: e01268.

Firmin JL, Wilson KE, Rossen L, Johnston AWB. 1986. Flavonoid activation of nodulation genes in *Rhizobium* reversed by other compounds present in plants. *Nature* **324**: 90–92.

Horvath B, Bachem CW, Schell J, Kondorosi A. 1987. Host-specific regulation of nodulation genes in Rhizobium is mediated by a plant-signal, interacting with the nodD gene product. *EMBO Journal* **6**: 841–848.

Ichimura M, Furuno T, Takahashi T, Dixon RA, Ayabe S. 1997. Enzymic O-methylation of isoliquiritigenin and licodione in alfalfa and licorice cultures. *Phytochemistry* **44**: 991–995.

Jardinaud MF, Boivin S, Rodde N, Catrice O, Kisiala A, Lepage A, Moreau S, Roux B, Cottret L, Sallet E *et al.* 2016. A laser dissection-RNAseq analysis highlights the activation of cytokinin pathways by NFs in the *Medicago truncatula* root epidermis. *Plant Physiology* **171**: 2256–2276.

Jiang S, Jardinaud MF, Gao J, Pecrix Y, Wen J, Mysore K, Xu P, Sanchez-Canizares C, Ruan Y, Li Q *et al.* 2021. NIN-like protein transcription factors regulate leghemoglobin genes in legume nodules. *Science* **374**: 625–628.

Kamboj DV, Bhatia R, Pathak DV, Sharma PK. 2010. Role of nodD gene product and flavonoid interactions in induction of nodulation genes in *Mesorhizobium ciceri*. *Physiology and Molecular Biology of Plants* **16**: 69–77.

Kelly S, Sullivan JT, Kawaharada Y, Radutoiu S, Ronson CW, Stougaard J. 2018. Regulation of Nod factor biosynthesis by alternative NodD proteins at distinct stages of symbiosis provides additional compatibility scrutiny. *Environmental Microbiology* **20**: 97–110.

Kosslak RM, Bookland R, Barkei J, Paaren HE, Appelbaum ER. 1987. Induction of *Bradyrhizobium japonicum* common *nod* genes by isoflavones isolated from *Glycine max*. *Proceedings of the National Academy of Sciences, USA* **84**: 7428–7432.

Lee E-Y, Chang I-H, Shin M-J, Cho H-J, Kim J-S, Eom J-E, Kwon Y, Na Y. 2011. chalcones as novel non-peptidic μ-calpain inhibitors. *Bulletin of the Korean Chemical Society* **32**: 3459–3464.

Letunic I, Bork P. 2021. Interactive Tree Of Life (iTOL) v5: an online tool for phylogenetic tree display and annotation. *Nucleic Acids Research* **49**(W1): W293–w296.

Li ZS, Alfenito M, Rea PA, Walbot V, Dixon RA. 1997. Vacuolar uptake of the phytoalexin medicarpin by the glutathione conjugate pump. *Phytochemistry* **45**: 689–693.

Libault M, Farmer A, Brechenmacher L, Drnevich J, Langley RJ, Bilgin DD, Radwan O, Neece DJ, Clough SJ, May GD *et al.* 2010. Complete transcriptome of the soybean root hair cell, a single-cell model, and its alteration in response to *Bradyrhizobium japonicum* infection. *Plant Physiology* **152**: 541–552.

Liu CW, Murray JD. 2016. The role of flavonoids in nodulation host-range specificity: an update. *Plants (Basel)* **5**: 33.

Liu H, Ding Y, Zhou Y, Jin W, Xie K, Chen LL. 2017. CRISPR-P 2.0: an improved CRISPR-Cas9 tool for genome editing in plants. *Molecular Plant* **10**: 530–532.

Liu Y, Fernie AR, Tohge T. 2022. Diversification of chemical structures of methoxylated flavonoids and genes encoding Flavonoid-*O*-Methyltransferases. *Plants (Basel)* **11**: 564.

Luu TB, Ourth A, Pouzet C, Pauly N, Cullimore J. 2022. A newly evolved chimeric lysin motif receptor-like kinase in *Medicago truncatula* spp. tricycla R108 extends its Rhizobia symbiotic partnership. *New Phytologist* **235**: 1995–2007.

Maxwell CA, Edwards R, Dixon RA. 1992. Identification, purification, and characterization of S-adenosyl-L-methionine: isoliquiritigenin 2'-*O*-methyltransferase from alfalfa (*Medicago sativa L.*). *Archives of Biochemistry and Biophysics* **293**: 158–166.

Maxwell CA, Harrison MJ, Dixon RA. 1993. Molecular characterization and expression of alfalfa isoliquiritigenin 2'-*O*-methyltransferase, an enzyme specifically involved in the biosynthesis of an inducer of *Rhizobium meliloti* nodulation genes. *The Plant Journal* **4**: 971–981.

Maxwell CA, Hartwig UA, Joseph CM, Phillips DA. 1989. A chalcone and two related flavonoids released from alfalfa roots induce *nod* genes of *Rhizobium meliloti*. *Plant Physiology* **91**: 842–847.

Maxwell CA, Phillips DA. 1990. Concurrent synthesis and release of *nod*-gene-inducing flavonoids from Alfalfa roots. *Plant Physiology* **93**: 1552–1558.

Mulligan JT, Long SR. 1985. Induction of *Rhizobium meliloti nodC* expression by plant exudate requires *nodD*. *Proceedings of the National Academy of Sciences, USA* **82**: 6609–6613.

Noel JP, Dixon RA, Pichersky E, Zubieta C, Ferrer JL. 2003. Structural, functional, and evolutionary basis for methylation of plant small molecules. In: Romeo JT, ed. *Recent advances in phytochemistry, vol. 37*. Amsterdam, the Netherlands: Elsevier, 37–58.

Peck MC, Fisher RF, Long SR. 2006. Diverse flavonoids stimulate NodD1 binding to nod gene promoters in *Sinorhizobium meliloti*. *Journal of Bacteriology* **188**: 5417–5427.

Phillips DA, Joseph CM, Maxwell CA. 1992. Trigonelline and stachydrine released from alfalfa seeds activate NodD2 protein in *Rhizobium meliloti*. *Plant Physiology* **99**: 1526–1531.

Pini F, East AK, Appia-Ayme C, Tomek J, Karunakaran R, Mendoza-Suarez M, Edwards A, Terpolilli JJ, Roworth J, Downie JA *et al.* 2017. Bacterial biosensors for *in vivo* spatiotemporal mapping of root secretion. *Plant Physiology* **174**: 1289–1306.

Quilbé J, Montiel J, Arrighi JF, Stougaard J. 2022. Molecular mechanisms of intercellular Rhizobial infection: novel findings of an ancient process. *Frontiers in Plant Science* **13**: 922982.

Radutoiu S, Madsen LH, Madsen EB, Jurkiewicz A, Fukai E, Quistgaard EM, Albrektsen AS, James EK, Thirup S, Stougaard J. 2007. LysM domains mediate lipochitin-oligosaccharide recognition and Nfr genes extend the symbiotic host range. *EMBO Journal* **26**: 3923–3935.

Schiessl K, Lilley JLS, Lee T, Tamvakis I, Kohlen W, Bailey PC, Thomas A, Luptak J, Ramakrishnan K, Carpenter MD *et al.* 2019. NODULE INCEPTION recruits the lateral root developmental program for symbiotic nodule organogenesis in *Medicago truncatula*. *Current Biology* **29**: 3657–3668.

Sousa C, Folch JL, Boloix P, Megias M, Nava N, Quinto C. 1993. A *Rhizobium tropici* DNA region carrying the amino-terminal half of a *nodD* gene and a nod-box-like sequence confers host-range extension. *Molecular Microbiology* **9**: 1157–1168.

Spaink HP, Wijffelman CA, Pees E, Okker RJH, Lugtenberg BJJ. 1987. *Rhizobium* nodulation gene nodD as a determinant of host specificity. *Nature* **328**: 337–340.

Stomp A-M. 1992. Histochemical localization of β-glucuronidase. In: Gallagher SR, ed. *GUS protocols: using the GUS gene as a reporter of gene expression*. San Diego, CA, USA: Academic Press Inc, 103–113.

Subramanian S, Stacey G, Yu O. 2006. Endogenous isoflavones are essential for the establishment of symbiosis between soybean and *Bradyrhizobium japonicum*. *The Plant Journal* **48**: 261–273.

Walker L, Lagunas B, Gifford ML. 2020. Determinants of host range specificity in legume-rhizobia symbiosis. *Frontiers in Microbiology* **11**: 3028.

Wang D, Dong W, Murray J, Wang E. 2022. Innovation and appropriation in mycorrhizal and rhizobial symbioses. *Plant Cell* **34**: 1573–1599.

Wang Q, Liu J, Zhu H. 2018. Genetic and molecular mechanisms underlying symbiotic specificity in legume-rhizobium interactions. *Frontiers in Plant Science* **9**: 313.

Wasson AP, Pellerone FI, Mathesius U. 2006. Silencing the flavonoid pathway in *Medicago truncatula* inhibits root nodule formation and prevents auxin transport regulation by rhizobia. *Plant Cell* **18**: 1617–1629.

Wen X, Walle T. 2006. Methylated flavonoids have greatly improved intestinal absorption and metabolic stability. *Drug Metabolism & Disposition* **34**: 1786–1792.

Xing HL, Dong L, Wang ZP, Zhang HY, Han CY, Liu B, Wang XC, Chen QJ. 2014. A CRISPR/Cas9 toolkit for multiplex genome editing in plants. *BMC Plant Biology* **14**: 327.

Yeh KC, Peck MC, Long SR. 2002. Luteolin and GroESL modulate *in vitro* activity of NodD. *Journal of Bacteriology* **184**: 525–530.

Zhang J, Subramanian S, Stacey G, Yu O. 2009. Flavones and flavonols play distinct critical roles during nodulation of *Medicago truncatula* by *Sinorhizobium meliloti*. *The Plant Journal* **57**: 171–183.

Zhang J, Subramanian S, Zhang Y, Yu O. 2007. Flavone synthases from *Medicago truncatula* are flavanone-2-hydroxylases and are important for nodulation. *Plant Physiology* **144**: 741–751.

Zhao J, Huhman D, Shadle G, He XZ, Sumner LW, Tang Y, Dixon RA. 2011. MATE2 mediates vacuolar sequestration of flavonoid glycosides and glycoside malonates in *Medicago truncatula*. *Plant Cell* **23**: 1536–1555.

Zubieta C, He XZ, Dixon RA, Noel JP. 2001. Structures of two natural product methyltransferases reveal the basis for substrate specificity in plant *O*-methyltransferases. *Nature Structural & Molecular Biology* **8**: 271–279.

Supporting Information

Additional Supporting Information may be found online in the Supporting Information section at the end of the article.

Fig. S1 *Sinorhizobium meliloti* carrying *pnodA*$_{Sm}$*:lux* shows no activity in response to flavonoids.

Fig. S2 Flavonoids used in this study and their chemical structures.

Fig. S3 A phylogenetic tree of 48 full-length *Medicago truncatula OMT*s.

Fig. S4 Clustering and phylogeny of *Medicago truncatula* MsChOMT homologs.

Fig. S5 *In vitro* activity of recombinant ChOMT1 using isoliquiritigenin as substrate.

Fig. S6 ChOMT1, ChOMT3 and GeOMT can methylate licodione.

Fig. S7 Isoliquiritigenin content of *chomt1*, *omt2* and *chomt1-3 omt2-2* double mutants.

Fig. S8 Nodulation phenotypes of *chomt1*, *omt2* and *chomt1-3 omt2-2* double mutants.

Fig. S9 Luminescence of detection of the *Sinorhizobium meliloti* 2011/pLMB830 bioreporter on nodulated and noninoculated plants, and without plants.

Table S1 Primers used in this study.

Table S2 All gene IDs and synonyms for genes in this study.

Please note: Wiley is not responsible for the content or functionality of any Supporting Information supplied by the authors. Any queries (other than missing material) should be directed to the *New Phytologist* Central Office.